Dual Axis and Single Axis Sun Tracking Maximal Energy Gain

Soulayman S.[1*], Hamoud M.[1]

[1] Applied Physics Department, Higher Institute for Applied Sciences and Technology, Damascus, Syria

Email Address

soulayman.soulayman@hiast.edu.sy (Soulayman S.), hamoudm92@gmail.com (Hamoud M.)
*Correspondence: soulayman.soulayman@hiast.edu.sy

Received: 12 December 2017**; Accepted:** 25 December 2017

Abstract:

The maximal possible energy gain in the case of dual axis and single axis sun tracking is calculated basing on Hottel clear sky radiation model (HM) and extraterrestrial solar radiation model (ESRM). An experimental setup was designed and constructed for theoretical results verification. It was found that, the maximum possible energy gain calculated basing on HM and ESRM are practically identic either with reference to the horizontal surface or with reference to arbitrary tilted surface. The experimental results show that HM and ESRM can be used for calculating the energy gain. For example, on 25 August from 8 O'clock to solar noon, the hourly energy gain values of HM and ESRM are 1.672, 1.336, 1.170, 1.098 and 1.097 while the corresponding measured values on the same day are 1.746, 1.36, 1.16, 1.043 and 1.027. Thus, the theoretical data are consistent with the measured ones. It is proved that, the tilt angle of the single axis tracked surface with reference to the horizon is equal to absolute value of difference between the latitude angle and the declination angle.

Keywords:

Sun Tracking, Single Axis, Dual Axis, Clear Sky, Hottel Model, Extraterrestrial Model, Experimental Results

1. Introduction

Photovoltaic energy involves the conversion of sunlight into electricity. The efficiency of converting radiant solar energy into electrical energy is the critical point that influences the choice of solar energy as a form of alternative energy. Photovoltaic (PV) systems have gained a great deal of interest in the world and these studies performed on this subject have been gaining more and more importance. The energy generated from PV modules is related with temperature, irradiance and incident angle of the solar radiation and so on. There are two ways to improve the PV technology performance. One is to use different materials or add other dopants to manufacture the PV modules. The other one is to use a tracker as the device for orienting a solar PV module toward the Sun. Simultaneous or short term tracking, where a device for orienting a solar PV module toward the Sun during the day is used. The efficiency of a PV module can easily be increased by sun tracking systems which are investigated by many researches. The generated power is directly proportional with the collected

solar radiation in a solar system. Maximum sun power collection is possible by adjusting solar system position with respect to the Sun's location. This adjustment can be realized more easily with two axes Sun tracking systems than single ones which is cheaper and simpler to design.

The tracking systems include closed and open loop control mechanisms. The PV modules are positioned by the help of photo sensors and feedback controllers. The disadvantage of the closed loop system is that the system spends more energy than the generated one in the case of quick weather changes. The open loop one is based on calculations of the seasonal weather and the sun position. The hybrid control is made up of both closed and open loop tracking systems [1].

Sun-tracking system plays an important role in the development of solar energy applications, especially for the high solar concentration systems that directly convert the solar energy into thermal or electrical energy. There are number of studies showing that tracking systems enable significant amount of solar energy compared to fixed systems. Nann [2] derived the irradiance received and the energy costs for tracking photovoltaic systems and V-trough concentrators relative to the costs of a fixed system. Tomson [3] reported increasing of seasonal energy yield by 10-20% if using the two-positional tracking system that positions collectors in the morning and in the afternoon. A very detailed review of energy gain of different trackers is done by Mousazadeh et al. [4] where the authors report a boost of collected solar energy by means of a tracking system in the range of 10-100% depending on different time periods and geographical conditions. However, Sun-tracking systems are quite expensive and energy intensive. An experimental study was performed by Abdallah [5] to investigate the effect of using different types of Sun tracking systems on the voltage–current characteristics and electrical power generation at the output of flat plate photovoltaics. The increment of electrical power gain was found to be up to 43.87%, 37.53%, 34.43% and 15.69% for the two axes, east–west, vertical and north–south tracking, respectively, as compared with the fixed surface inclined 32 ° to the south in Amman, Jordan.

Two most commonly used configurations in two-axis sun-tracking system are azimuth-elevation and tilt-roll (or polar) tracking system. The azimuth-elevation system is among the most popular sun-tracking system employed in various solar energy applications [6]. In the azimuth-elevation tracking, the collector must be free to rotate about the zenith-axis and the axis parallel to the surface of the earth. The tracking angle about the zenith-axis is the solar azimuth angle and the tracking angle about the horizontal axis is the solar elevation angle. Alternatively, tilt-roll (or polar) tracking system adopts an idea of driving the collector to follow the sun-rising in the east and sun-setting in the west from morning to evening as well as changing the tilting angle of the collector due to the yearly change of sun path [7, 8]. Hence, for the tilt-roll tracking system, one axis of rotation is aligned parallel with the earth's polar-axis that is aimed towards the star Polaris. This gives it a tilt from the horizon equal to the local latitude angle. The other axis of rotation is perpendicular to this polar-axis [9, 10]. The tracking angle about the polar-axis is equal to the sun's hour angle and the tracking angle about the perpendicular axis is dependent on the declination angle.

Hottel [11] presented a model, with a good accuracy and simple use, to estimate the clear-day transmittance of direct solar radiation through clear sky. Basing on this model, it is possible to calculate the solar irradiance $G(n)$ at horizontal and tilted surfaces of different orientations. In this general model, with taking into account the

solar zenith θ_z angle and cite altitude A the transmittance to direct solar radiation could be calculated using constants and corrections for four different climate zones in the globe (see [11]). Thus, this model could be used for calculating the energy gain of the tracked surface with respect to tilted and horizontal surfaces. Soulayman and Sabbagh [12] proposed a method for calculating extraterrestrial solar radiation at surfaces with different tilts and orientations. This method was used for calculating the energy gain of tilted surfaces with respect to horizontal and fixed tilted surfaces [13]. Thus, it could be used for calculating the energy gain of the tracked surfaces.

The different sun tracking systems are a subject of various research projects for a variety of applications. Yinghao et al [14] implemented a sun tracking imaging system for minimizing circumsolar image distortion for improved short-term solar irradiance forecasts. Abdelghani-Idrissi et al [15] used sun tracking for enhancing the thermal efficiency of a solar water heating system. The solar tracker shows a 49% gain of overall stored thermal energy. Mirzaei and Mohiabadi [16] built three single axis sun trackers, performing in three different tracking modes, and coupled them with PV modules to measure the power generation of the solar PV system in the semi-arid climatic characteristics of Rafsanjan, Iran. Maatallah et al [17] investigated the performance of a novel solar energy concentrating system consisting of a cylindrical mirror placed in a stationary position and a receiver tracking system. Fadhel et al [18] investigated, experimentally, the solar drying of Tunisian phosphate in the open sun, under greenhouse and by a parabolic dish concentrator. They showed that, the drying by the parabolic dish concentrator gives results whose perspectives are satisfactory compared with the drying in the open sun or under greenhouses. Simoni Perini et al [19] investigated dual-axis tracking linear Fresnel lenses concentrated solar thermal collector theoretically and experimentally. They mentioned that, an evacuated receiver could increase the global efficiency up to 55%. Bone et al [20] investigated the intra-hour direct normal irradiance forecasting through adaptive clear-sky modeling and cloud tracking. They found that, over all test days, the adaptive method has an average root mean square error of 3.06%, which represents a 19% improvement over the same method that uses the optimal model parameters from the previous day's data.

The economic feasibility of different tracking systems is a subject of several articles. Sharaf Eldin et al [21] mentioned that, the energy generated by tracking the sun is not feasible in hot countries. Arian Bahrami et al [22] studied the technical and economic assessment of fixed, single and dual-axis tracking PV panels in low latitude countries. They mentioned that, the performance of the solar trackers in terms of the energy gain and levelized cost of electricity (LCOE) in Nigeria is ranked to show the most preferred option for implementation. Bakhshi and Sadeh [23] proposed a comprehensive economic analysis method for selecting the PV array structure in grid–connected photovoltaic systems. The performance of the suggested algorithm is evaluated through a commercial dual axis GCPV system simulation.

Different concepts of sun tracking are treated also widely. Chiesi, et al [24] investigated the effect of tracking errors in heliostats used in solar tower power plants and proposed an approach based on low-cost distributed electronics capable of limiting their impact. Fathabadi [25] proposed an offline sensorless dual-axis solar tracker for using in photovoltaic systems and solar concentrators and mentioned that, the concept is experimentally verified and found that, 19.1%–30.2% more solar energy can be captured depending on the seasons by utilizing the tracker. A novel gravity based passive solar tracking mechanism; suitable to a linear solar concentrating collector has been conceptualized, developed, simulated, analyzed and

tested experimentally [26]. Lu and Hajimirza [27] proposed a numerical model to estimate dust accumulation on the surface of a two-dimensional panel, in which the adsorption/desorption rate of airborne dust under the effect of gravity and other dust-panel interaction (i.e., Van der Waals and electrostatic effects) can be calculated. Optimization results showed that by applying the proposed optimal tilt angle adjustment protocol, the daily absorption efficiency of a silicon solar panel can be improved by up to 24% depending on the friction coefficient compared to the dual-axis solar tracking system.

In the present work a tracking system which could be either one axis or dual axis is described and the energy gain of the tracked system is evaluated with regard to horizontal, latitude tilted, daily optimum tilted, monthly optimum tilted, seasonally optimum tilted and biannually optimum tilted solar PV modules.

2. Materials and Methods

The motive behind this work is to design an automatic sun tracker which can work as a dual axis or single axis. The function of the tracker is to make the PV module extract maximum possible amount of solar energy and convert it to electrical energy. The sun tracker should consume energy as minimum as possible.

2.1. Experimental Setup

In constructing the sun tracker, see Figure 1, four LDRs were used to achieve the optimum orientation of the PV module using two DC motors with consumption 0.3A at 12V each through the microcontroller (pic16877A). A rechargeable battery was used to store the power and to feed the tracker at the end of the day. Kipp & Zonen pyranometers were used to measure solar radiation incident on the fixed and tracked modules. Pt-100 sensors were used for measuring ambient and surface module's temperatures. Data logger is used to collect data over a period of time.

The experimental setup is performed with a meteorological station on the roof of the applied physics department at Higher Institute for Applied Sciences and Technology, Damascus (33.5^{o}N, 36.3^{o}E), Syria, where all solar radiation components are measured all over the day.

The measured data such as PV panel's current intensity I and voltage V, solar radiation intensity on the plane of the PV panel, PV panel's surface temperature, ambient temperature, PV panel's surface azimuth and tilt angles, are collected using an indoor arrangement where the data logger is the main component (see Figure 2).

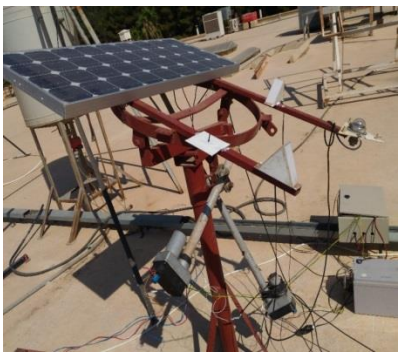

Figure 1. *Dual and single axis sun tracker.*

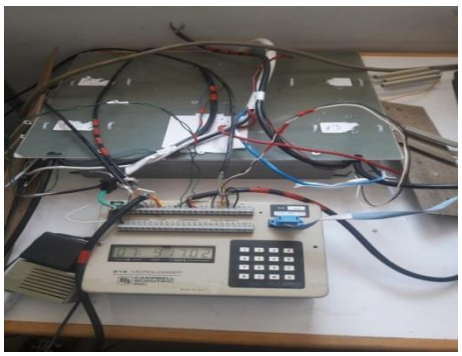

Figure 2. *Data collection unit.*

2.2. Dual Axis Energy Gain Theory

Let us consider the ideal case - the ideal instantaneous dual tracking. In this case the incidence angle satisfies the following equation:

$$\theta_i = 0^o \tag{1}$$

Thus, the daily extraterrestrial solar radiation $H_{0,d}(n)$, incident on ideal tracked surface, on a day number n, in this case, is:

$$H_{0,d}(n) = G_s(n).S_0(n) \tag{2}$$

where $S_0(n)$ is the maximum possible sunshine duration (day length) during the day number n, G_s could be obtained, for nth day number in the year, from the following equation:

$$G_s(n) = I_s * \begin{Bmatrix} 1.00011 + 0.034221\, cos(B_n) \\ +0.00128\, sin(B_n) + 0.000719 cos(B_n) \\ +0.000077 * sin(B_n) \end{Bmatrix} \tag{3}$$

where I_s is the solar constant $I_s = 1367 W/m^2$ and $B_n = 2\pi(n-1)/365$.

When dividing the value of the equation (2) by the value of the daily extraterrestrial solar radiation on the horizontal plane, the energy gain factor of daily instantaneous dual tracking with relation to horizontal surface could be obtained as follows:

$$R = \left[H_{0,d}(n, \theta_i = 0^o)/H_{0,d}(n, \theta_i variable)\right] =$$
$$\frac{2}{15} arccos(-tg\varphi tg\delta) \Big/ \begin{bmatrix} cos\varphi cos\delta sin\omega_s \\ +\frac{\pi * \omega_s}{180} sin\varphi sin\delta \end{bmatrix} \tag{4}$$

where ω_s is the sunset hour angle on a horizontal surface, δ is the declination angle and φ is the geographic latitude of the site. On the other hand, the energy gain factor of daily instantaneous dual tracking with relation to Equator facing tilted surface by an angle β could be obtained as:

$$R' = \left[H_{0,d}(n, \theta_i = 0^o)/H_{0,d}(n, \beta)\right] =$$
$$\left\{\frac{2}{15} arccos(-tg\varphi tg\delta) \Big/ \begin{bmatrix} cos(\varphi - \beta) cos\delta sin\omega_{ss} \\ +\frac{\pi * \omega_{ss}}{180} sin(\varphi - \beta) sin\delta \end{bmatrix}\right\} \tag{5}$$

where ω_{ss} is the sunset hour angle on a tilted surface. Basing on the equations (4) and (5) it possible to introduce instantaneous and hourly energy gain factor of R_1 and R_2. The instantaneous dual tracking energy gain with relation to horizontal surface could be obtained as follows:

$$R_1 = [G(n, \theta_i = 0^o)/G_0(n, \theta_i variable)] =$$
$$\begin{bmatrix} cos\varphi cos\delta cos\omega \\ +sin\varphi sin\delta \end{bmatrix}^{-1} \tag{6}$$

where ω is the hour angle. The hourly energy gain factor of instantaneous dual tracking with relation to horizontal surface could be obtained as follows:

$$R_2 = \left[H_h(n, \theta_i = 0^o)/H_{0,h}(n, \theta_i variable)\right] =$$
$$\begin{bmatrix} cos\varphi cos\delta(sin\omega_2 - sin\omega_1) \\ +\pi sin\varphi sin\delta(\omega_2 - \omega_1)/180 \end{bmatrix}^{-1} \tag{7}$$

where ω_1 and ω_2 are the hour angles of the beginning and ending of the hour in consideration respectively. On the other hand, the energy gain factor of daily instantaneous dual tracking with relation to Equator facing tilted surface by an angle β could be obtained as:

$$R_3 = [H_d(n,\theta_i = 0^o)/H_d(n,\beta)] = \begin{bmatrix} cos(\varphi-\beta)cos\delta(sin\omega_2 - sin\omega_1) \\ +\pi sin(\varphi-\beta)sin\delta(\omega_2-\omega_1)/180 \end{bmatrix}^{-1} \quad (8)$$

2.3. Single Axis Energy Gain Theory

Contrary to ideal instantaneous dual axis tracking, the incidence angle is not zero, but the tilt angle β_{tr} of the surface with respect to horizon is constant. In order to reach the maximum possible energy gain β_{tr} should be optimized. For a plane with a fixed slope rotated about a vertical axis, the angle of incidence is minimized when the surface azimuth γ and solar azimuth γ_s angles are equal. In this case, incidence angle satisfies the following equation:

$$cos\,\theta_i = cos(\theta_z - \beta_{tr}) \quad (9)$$

where θ_z is the solar zenith angle. Thus, the instantaneous extraterrestrial solar radiation $G_{0,f}(n)$, incident on single axis tracked surface, on a day number n, in this case, is:

$$G_{0,f}(n) = G_s(n).cos\,\theta_i \quad (10)$$

When dividing the value of the equation (10) by the value of the instantaneous extraterrestrial solar radiation on the horizontal plane, the instantaneous energy gain factor of single axis tracking with relation to horizontal surface could be obtained as follows:

$$R_4 = \frac{cos\,\theta_i}{cos\,\theta_z} \quad (11)$$

On the other hand, the hourly energy gain factor of single axis tracking with relation to horizontal surface could be obtained as:

$$R_5 = \cos\left[\theta_i\left(\frac{\omega_2+\omega_1}{2}\right)\right]\begin{bmatrix} cos\varphi cos\delta(sin\omega_2 - sin\omega_1) \\ +\pi(\omega_2-\omega_1)sin\varphi sin\delta/180 \end{bmatrix}^{-1} \quad (12)$$

and the energy gain factor of single axis tracking with relation to Equator facing tilted surface by any angle β could be obtained as:

$$R_6 = \cos\left[\theta_i\left(\frac{\omega_2+\omega_1}{2}\right)\right]\begin{bmatrix} cos(\varphi-\beta)cos\delta(sin\omega_2 - sin\omega_1) \\ +\pi sin(\varphi-\beta)sin\delta(\omega_2-\omega_1)/180 \end{bmatrix}^{-1} \quad (13)$$

With reference to the equation (9) it is reasonable to mention that, as β_{tr} is constant all over the day and it changes from one day to another one, it is possible to determine its value at solar noon when the hour angle is 0^o. At this moment, the incident angle is zero and the zenith angle satisfies the following equation:

$$\theta_z = \varphi - \delta \quad (14)$$

This means that,

$$\beta_{tr} = \varphi - \delta \quad (15)$$

where the declination angle δ could be calculated using the Copper formula [28]:

$$\delta = 23.45sin\left[\frac{2\pi(n+284)}{365}\right] \quad (16)$$

Equation (15) was given for the first time by Stanciu and Stanciu [29] for predicting the optimum tilt angle for flat plate collectors all over the world. This formula was commented by Soulayman [30].

3. Results and Discussion

3.1. Extraterrestrial Solar Radiation Model Results

When calculting the hourly energy gain of dual axis tracking R_2 at Damascus (33.5^oN, 36.3^oE), basing on extraterrestrial method, at vernal equinox, winter and summer solstices using the equation (7), the results of calculations are given in Table 1. It is seen from Table 1 that, the dual tracking with respect to horizontal surface is minimal during midday hours from 10:30 to 13:30 solar time while it becomes more and more important when approaching sunrise and sunset. Therefore, the use of dual axis tracking mode allows effectively use the solar radiation early morning and afternoon with regard to fixed tilted surfaces.

Table 1. *Energy gain of dual axis tracked surface with relation to horizontal surface during vernal equinox, winter and summer solstices at Damascus (33.5^oN, 36.3^oE).*

hr	Vernal equinox	Summer solstice	Winter solstice
5.5		8.35	
6.5	9.62	3.13	
7.5	3.18	1.95	13.68
8.5	1.99	1.46	4.06
9.5	1.52	1.21	2.58
10.5	1.31	1.08	2.05
11.5	1.22	1.02	1.86
12.5	1.22	1.02	1.86
13.5	1.31	1.08	2.05
14.5	1.52	1.21	2.58
15.5	1.99	1.46	4.06
16.5	3.18	1.95	13.68
17.5	9.62	3.13	
18.5		8.35	

When applying the same algorithm for calculting the hourly energy gain of dual axis tracking R_2 at other cities such as Luxur (25.6872 ° N, 32.6396 ° E), Rome (41.9028 ° N, 12.4964 ° E) and Copenhagen (55.6761 ° N, 12.5683 ° E), the results are presented in Tables 2 to 4. It is seen from Tables 2 to 4 that, the energy gain decreases with decreasing the cite latitude and the observed hourly behavior of R_2 during the day is observed also. Therefore, the tracking becomes more and more important with increasing the cite latitude.

Table 2. *Energy gain of dual axis tracked surface with relation to horizontal surface during vernal equinox, winter and summer solstices at Luxur.*

hr	Vernal equinox	Summer solstice	Winter solstice
5.5		15.64	
6.5	8.78	3.57	
7.5	2.93	2.05	6.91
8.5	1.83	1.48	3.01
9.5	1.41	1.21	2.06
10.5	1.21	1.07	1.69
11.5	1.12	1.01	1.54
12.5	1.12	1.01	1.54
13.5	1.21	1.07	1.69

14.5	1.41	1.21	2.06
15.5	1.83	1.48	3.01
16.5	2.93	2.05	6.91
17.5	8.78	3.57	
18.5		15.64	

Table 3. *Energy gain of dual axis tracked surface with relation to horizontal surface during vernal equinox, winter and summer solstices at Rome.*

hr	Vernal equinox	Summer solstice	Winter solstice
4.5		284.7	
5.5		5.68	
6.5	10.94	2.82	
7.5	3.58	1.9	
8.5	2.23	1.47	6.62
9.5	1.71	1.24	3.61
10.5	1.46	1.11	2.73
11.5	1.36	1.06	2.42
12.5	1.36	1.06	2.42
13.5	1.46	1.11	2.73
14.5	1.71	1.24	3.61
15.5	2.23	1.47	6.62
16.5	3.58	1.9	
17.5	10.94	2.82	
18.5		5.68	
19.5		284.7	

Table 4. *Energy gain of dual axis tracked surface with relation to horizontal surface during vernal equinox, winter and summer solstices at Copenhagen.*

hr	Vernal equinox	Summer solstice	Winter solstice
3.5		78.05	
4.5		7.69	
5.5		3.84	
6.5	15.04	2.53	
7.5	4.79	1.9	
8.5	2.97	1.55	
9.5	2.27	1.35	12.07
10.5	1.94	1.24	6.64
11.5	1.81	1.19	5.39
12.5	1.81	1.19	5.39
13.5	1.94	1.24	6.64
14.5	2.27	1.35	12.07
15.5	2.97	1.55	
16.5	4.79	1.9	
17.5	15.04	2.53	
18.5		3.84	
19.5		7.69	
20.5		78.05	

3.2. Experimental Verification of ESMR Results

When calculating and measuring the radiation gain on two clear days (day number 277 and day number 288), the results presented in Figure 3 are obtained. It is seen from Figure 3 that, the agreement between theoretical and experimental results is very good. Moreover, the tracking effect on the radiation gain is important outside the

midday hours (from 11:30 to 13:30) and it becomes greater and greater when approaching sunrise and sunset.

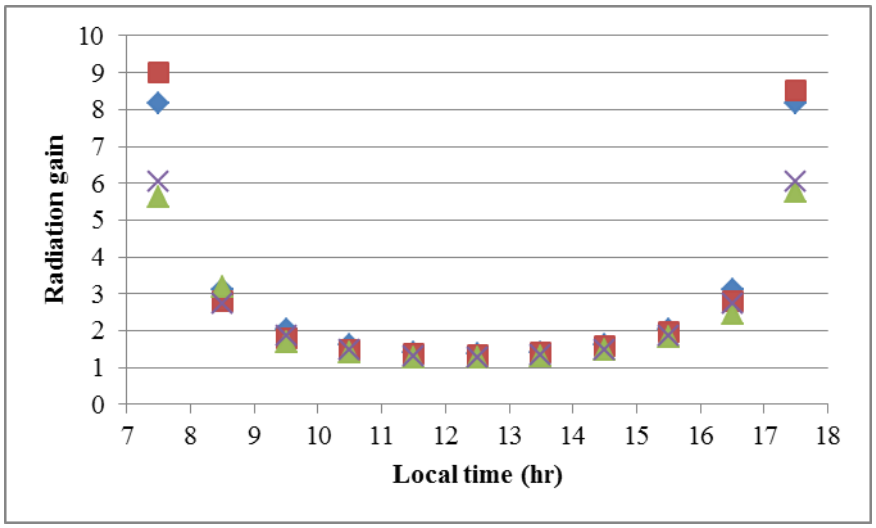

Figure 3. *The calculated (x and ■) and measured (▲and ♦) radiation gain on day numbers 277 and 288 respectively.*

3.3. Dual Axis and Single Axis Tracking Energy Gain

In order to have an idea about the orientation angles of dual axis and single axis tracking surfaces it is important to present the values of these angles at four characteristic days (vernal equinox, summer solstice, autumnal equinox and winter solstice) at a definite site. Table 5 presents these values for vernal equinox and summer solstice while Table 6 presents these values for autumnal equinox and winter solstice at Damascus (33.5^{o}N, 36.3^{o}E). It is clearly demonstrated that, the azimuth angle of the tracked surface γ_{tr} is the same for both tracking mode while the optimum tilt of the single axis tracked surface is determined using equation (15). Moreover, when doing the same calculations for Luxur (25.6872 ° N, 32.6396 ° E) and Copenhagen (55.6761 °N, 12.5683 °E), the results are given in the Tables 7 and 8. It is clear from Tables 7 and 8 that, as γ_{tr} has the same values for both tracking modes, a single column for both modes is included. Moreover, the optimum tilt angle of the single axis mode is lower than all hourly values of the dual axis tilt mode.

Table 5. *Tracked surface orientation angles on vernal equinox and summer solstice.*

	Vernal equinox				**Summer solstice**			
	β_{tr}		**γ_{tr}**		**β_{tr}**		**γ_{tr}**	
hr	**Single**	**dual**	**Single**	**dual**	**Single**	**dual**	**Single**	**dual**
4.5					10.1	-	-121.8	-121.8
5.5					10.1	83.1	-113.6	-113.6
6.5	34	84.0	-89.58	-89.58	10.1	71.4	-106.3	-106.3
7.5	34	71.7	-81.16	-81.16	10.1	59.2	-99.3	-99.3
8.5	34	59.8	-71.89	-71.89	10.1	46.7	-91.9	-91.9
9.5	34	49.0	-60.65	-60.65	10.1	34.3	-82.9	-82.9
10.5	34	40.1	-45.85	-45.85	10.1	22.1	-68.8	-68.8
11.5	34	34.7	-25.59	-25.59	10.1	12.0	-35.1	-35.1
12.5	34	34.7	0	0	10.1	12.0	35.1	35.1
13.5	34	40.1	25.59	25.59	10.1	22.1	68.8	68.8
14.5	34	49.0	45.85	45.85	10.1	34.3	82.9	82.9
15.5	34	59.8	60.65	60.65	10.1	46.7	91.9	91.9

16.5	34	71.7	71.89	71.89	10.1	59.2	99.3	99.3
17.5	34	84.0	81.16	81.16	10.1	71.4	106.3	106.3
18.5					10.1	83.1	113.6	113.6
19.5					10.1	-	121.8	121.8

Table 6. *Tracked surface orientation angles on autumnal equinox and winter solstice.*

	Autumnal equinox				**Winter solstice**			
	β_{tr}		**γ_{tr}**		**β_{tr}**		**γ_{tr}**	
hr	**Single**	**dual**	**Single**	**dual**	**Single**	**dual**	**Single**	**dual**
6.5	33.6	83. 8	-85.8	-85.8				
7.5	33.6	71.4	-77.1	-77.1	56.9	85.81	-58.2	-58.2
8.5	33.6	59.5	-67	-67	56.9	75.75	-48. 7	-48. 7
9.5	33.6	48.6	-54.2	-54.2	56.9	67.21	-37.3	-37.3
10.5	33.6	39.7	-36.8	-36.8	56.9	60.85	-23.7	-23.7
11.5	33.6	34.3	-13.4	-13.4	56.9	57.4	-8.2	-8.2
12.5	33.6	34.3	13.4	13.4	56.9	57.4	8.2	8.2
13.5	33.6	39.7	36.8	36.8	56.9	60.85	23.7	23.7
14.5	33.6	48.6	54.2	54.2	56.9	67.21	37.3	37.3
15.5	33.6	59.5	67	67	56.9	75.75	48. 7	48. 7
16.5	33.6	71.4	77.1	77.1	56.9	85.81	58.2	58.2
17.5	33.6	83. 8	85.8	85.8				

Table 7. *Tracked surface orientation angles at Luxur.*

	Vernal equinox			**Summer solstice**			**Winter solstice**		
	β_{tr}		**γ_{tr}**	**γ_{tr}**	**β_{tr}**		**γ_{tr}**	**β_{tr}**	
hr	**Single**	**dual**			**Single**	**dual**		**Single**	**dual**
5.5				-114.3	2.2	86.33			
6.5	26.1	83.46	-86.29	-108.66	2.2	73.74			
7.5	26.1	70.04	-79.38	-103.74	2.2	60.75	-58.94	49	81.68
8.5	26.1	56.96	-71.14	-99.17	2.2	47.5	-50.49	49	70.63
9.5	26.1	44.63	-60.05	-94.54	2.2	34.07	-39.67	49	61.02
10.5	26.1	33.97	-43.23	-88.8	2.2	20.56	-25.84	49	53.67
11.5	26.1	27.09	-16.65	-74.09	2.2	7.15	-9.05	49	49.58
12.5	26.1	27.09	16.65	74.09	2.2	7.15	9.05	49	49.58
13.5	26.1	33.97	43.23	88.8	2.2	20.56	25.84	49	53.67
14.5	26.1	44.63	60.05	94.54	2.2	34.07	39.67	49	61.02
15.5	26.1	56.96	71.14	99.17	2.2	47.5	50.49	49	70.63
16.5	26.1	70.04	79.38	103.74	2.2	60.75	58.94	49	81.68
17.5	26.1	83.46	86.29	108.66	2.2	73.74			
18.5				114.3	2.2	86.33			

Table 8. *Tracked surface orientation angles at Copenhagen.*

	Vernal equinox			**Summer solstice**			**Winter solstice**		
	β_{tr}		**γ_{tr}**	**γ_{tr}**	**β_{tr}**		**γ_{tr}**	**β_{tr}**	
hr	**Single**	**dual**			**Single**	**dual**		**Single**	**dual**
3.5				-133.29	32.2	89.27			
4.5				-121.26	32.2	82.53			
5.5				-109.59	32.2	74.89			
6.5	56.1	86.19	-83.52	-97.89	32.2	66.67			
7.5	56.1	77.94	-70.86	-85.62	32.2	58.22			

8.5	56.1	70.33	-57.41	-72.03	32.2	49.92			
9.5	56.1	63.84	-42.71	-56.07	32.2	42.31	-34.08	79	85.25
10.5	56.1	59.02	-26.51	-36.5	32.2	36.18	-20.8	79	81.34
11.5	56.1	56.44	-9.01	-12.83	32.2	32.63	-7	79	79.31
12.5	56.1	56.44	9.01	12.83	32.2	32.63	7	79	79.31
13.5	56.1	59.02	26.51	36.5	32.2	36.18	20.8	79	81.34
14.5	56.1	63.84	42.71	56.07	32.2	42.31	34.08	79	85.25
15.5	56.1	70.33	57.41	72.03	32.2	49.92			
16.5	56.1	77.94	70.86	85.62	32.2	58.22			
17.5	56.1	86.19	83.52	97.89	32.2	66.67			
18.5				109.59	32.2	74.89			
19.5				121.26	32.2	82.53			
20.5				133.29	32.2	89.27			

When calculating the hourly energy gains, R_2 and R_5, of the both tracking modes with reference to the horizontal surface at Damascus during the same characteristic days, results presented in Table 5 are obtained. It is seen from Table 9 that, on the midday of the summer solstice **the energy gain of single axis tracking is approximately 1 while the energy gain of the dual mode is always sufficiently greater than 1.**

Table 9. *Hourly tracking modes energy gain at Damascus at characteristic days.*

	Vernal equinox		**Summer solstice**		**Autumnal equinox**		**Winter solstice**	
hr	**R_2**	**R_5**	**R_2**	**R_5**	**R_2**	**R_5**	**R_2**	**R_5**
5.5			8.35	2.43				
6.5	9.62	6.18	3.13	1.5	9.23	5.9		
7.5	3.18	2.52	1.95	1.28	3.14	2.48	13.68	11.98
8.5	1.99	1.79	1.46	1.17	1.97	1.77	4.06	3.85
9.5	1.52	1.47	1.21	1.1	1.51	1.46	2.58	2.54
10.5	1.31	1.3	1.08	1.06	1.3	1.29	2.05	2.05
11.5	1.22	1.22	1.02	1.02	1.21	1.21	1.86	1.86
12.5	1.22	1.22	1.02	1.02	1.21	1.21	1.86	1.86
13.5	1.31	1.3	1.08	1.06	1.3	1.29	2.05	2.05
14.5	1.52	1.47	1.21	1.1	1.51	1.46	2.58	2.54
15.5	1.99	1.79	1.46	1.17	1.97	1.77	4.06	3.85
16.5	3.18	2.52	1.95	1.28	3.14	2.48	13.68	11.98
17.5	9.62	6.18	3.13	1.5	9.23	5.9		
18.5			8.35	2.43				

3.4. Hottel Clear Sky Radiation Model Results

When applying Hottel [11] model (HM) for calculating the instantaneous and hourly energy gains R_1 to R_6 at Damascus (33.5^{o}N, 36.3^{o}E), it was found that, HM results are practically identic to ESRM ones. This means that, HM and ESRM models are equivalent in calculating the energy gain.

4. Conclusions

Finally, one can mention that, HM and ESRM models are effective and acceptable in calculating the energy gain. These models are totally equivalent in calculating the energy gain. The optimum tilt of the single axis tracked surface should be determined first before applying this mode using programmed mechanical systems. Moreover, one can conclude the following:

The optimum tilt of the single axis tracker could be determined simply basing on declination and latitude angles.

For the first time equation (15) is proposed for determining the optimum tilt of the single axis tracker.

The optimum tilt of the single axis tracker is always lower than the hourly values of the dual axis tracker's tilt angle.

The energy gain becomes greater and greater with increasing the latitude.

Conflicts of Interest

The authors declare that there is no conflict of interest regarding the publication of this article.

Nomenclature

β Tilt angle (^{o}) which is positive for equator facing case and negative for Pole facing cases

$\beta_{opt,b}$ Biannually optimum tilt angle (^{o})

$\beta_{opt,d}$ Daily optimum tilt angle (^{o})

$\beta_{opt,m}$ Monthly optimum tilt angle (^{o})

$\beta_{opt,s}$ Seasonally optimum tilt angle (^{o})

$\beta_{opt,y}$ Yearly optimum tilt angle (^{o})

β_{tr} Tracked surface tilt angle (^{o})

δ Solar declination angle (^{o})

γ Surface azimuth angle (^{o})

γ_s Sun azimuth angle (^{o})

γ_{tr} Tracked surface azimuth angle (^{o})

G Solar radiation intensity on a tilted surface (W/m^2)

G_o Solar radiation intensity on a horizontal surface (W/m^2)

G_s Solar radiation intensity outside Earth's atmosphere (W/m^2)

H Monthly average daily solar radiation on a horizontal surface (MJ/m^2)

H_d Daily solar radiation on a tilted surface (MJ/m^2)

$H_{d,o}$ Daily solar radiation on a horizontal surface (MJ/m^2)

H_0,d Daily extraterrestrial solar radiation on a horizontal surface (MJ/m^2)

I_s Solar constant (W/m^2)

n Day number in the year starting from January 1st

R Geometric tilt factor with respect to horizontal surface

R' Geometric tilt factor with respect to tilted surface

R_1 Instantaneous dual axis tracking energy gain with relation to horizontal surface

R_2 Hourly energy gain of instantaneous dual axis tracking with relation to horizontal surface

R_3 Hourly energy gain of instantaneous dual axis tracking with relation to tilted

surface

R_4 Instantaneous single axis tracking energy gain with relation to horizontal surface

R_5 Hourly energy gain of instantaneous single axis tracking with relation to horizontal surface

R_6 Hourly energy gain of instantaneous single axis tracking with relation to tilted surface

S_o Maximum possible sunshine duration (hr)

φ Latitude (^{o}) which is positive at NH and negative at SH

θ_i Solar rays incidence angle (^{o})

θ_z Solar zenith angle (^{o})

ω_s Sunset hour angle at a horizontal surface (^{o})

ω_{ss} Sunset hour angle at a tilted surface (^{o})

References

[1] Seme, S.; Stumberger, G. A novel prediction algorithm for solar angles using solar radiation and Differential Evolution for dual-axis sun tracking purposes. *Solar Energy*, 2011, 85(11), 2757-2770.

[2] Nann, S. Potentials for tracking photovoltaic systems and V-troughs in moderate climates. *Solar Energy*, 1990, 45(6), 385-393.

[3] Tomson, T. Discrete two-positional tracking of solar collectors. *Renewable Energy*, 2008, 33(3), 400-405.

[4] Mousazadeh, H.; Keyhani, A.; Javadi, A.; Mobli, H.; Abrinia, K.; Sharifi, A. A review of principle and Sun-tracking methods for maximizing solar systems output. *Renewable and Sustainable Energy Reviews*, 2009, 13(8), 1800-1818.

[5] Abdallah, S. The effect of using Sun tracking systems on the voltage-current characteristics and power generation of at plate photovoltaics. *Energy Conversion and Management*, 2004, 45 (11-12), 1671-1679.

[6] Roth, P.; Georgiev, A.; Boudinov, H. Design and construction of a system for sun-tracking. *Renewable Energy*, 2004, 29(3), 393-402.

[7] Nuwayhid, R.Y.; Mrad, F.; Abu-Said, R. The realization of a simple solar tracking concentrator for the university research applications. *Renewable Energy*, 2001, 24(2), 207-222.

[8] Sharan, A.M.; Prateek, M. Automation of minimum torque-based accurate solar tracking systems using microprocessors. *Journal of Indian Institute of Science*, 2006, 86(5), 415-437.

[9] Poulek, V.; Libra, M. New solar tracker. *Solar Energy Materials & Solar Cells*, 1998, 51(2), 113-120.

[10] Poulek, V.; Libra, M. A very simple solar tracker for space and terrestrial applications. *Solar Energy Materials & Solar Cells*, 2000, 60 (2), 99-103.

[11] Hottel, H.C. A simple model for estimating the transmittance of direct solar radiation through clear atmospheres. *Solar Energy*, 1976, 18(2), 129-134.

[12] Soulayman, S.; Sabbagh, W. Comment on 'Optimum tilt angle and orientation for solar collectors in Syria' by Skeiker, K. *Energy Conversion and Management*, 2015, 89, 1001-1002.

[13] Soulayman, S.; Hammoud, M. Optimum tilt angle of solar collectors for building applications in mid-latitude zone. *Energy Conversion Management*, 2016, 124, 20-28.

[14] Yinghao Chu; Mengying Li; Carlos F.M. Coimbra Sun-tracking imaging system for intra-hour DNI forecasts. *Renewable Energy*, 2016, 96, Part A, 792-799.

[15] Abdelghani-Idrissi, M.A.; Khalfallaoui, S.; Seguin, D.; Verniè res-Hassimi, L.; Leveneur, S. Solar tracker for enhancement of the thermal efficiency of solar water heating system. *Renewable Energy*, 2018, 119, 79-94.

[16] Mirzaei, M.; Mohiabadi, M.Z. Comparative Analysis of Energy Yield of Different Tracking Modes of PV Systems in Semiarid Climate Conditions: the Case of Iran. *Renewable Energy*, 2018, 119, 400-409.

[17] Maatallah, T.; Houcine, A.; El Alimi, S.; Ben Nasrallah, S. A novel solar concentrating system based on a fixed cylindrical reflector and tracking receiver. *Renewable Energy*, 2018, 117, 85-107.

[18] Fadhel, A.H.; Charfi, K.; Balghouthi, M.; Kooli, S. Experimental investigation of the solar drying of Tunisian phosphate under different conditions. *Renewable Energy*, 2018, 116, Part A, 762-774.

[19] Simoni Perini; Xavier Tonnellier; Peter King; Christopher Sansom, Theoretical and experimental analysis of an innovative dual-axis tracking linear Fresnel lenses concentrated solar thermal collector. *Solar Energy*, 2017, 153, 679-690.

[20] Bone, V.; Pidgeon, J.; Kearney, M.; Veeraragavan, A. Intra-hour direct normal irradiance forecasting through adaptive clear-sky modelling and cloud tracking. *Solar Energy*, 2018, 159, 852-867.

[21] Sharaf Eldin, S.A.; Abd-Elhady, M.S.; Kandil, H.A. Feasibility of solar tracking systems for PV panels in hot and cold regions. *Renewable Energy*, 2016, 85, 228-233.

[22] Arian Bahrami; Chiemeka Onyeka Okoye; Ugur Atikol. Technical and economic assessment of fixed, single and dual-axis tracking PV panels in low latitude countries. *Renewable Energy*, 2017, 113, 563-579.

[23] Bakhshi, R.; Sadeh, J.A. comprehensive economic analysis method for selecting the PV array structure in grid–connected photovoltaic systems. *Renewable Energy*, 2016, 94, 524-536.

[24] Chiesi, M.; Scarselli, E.F.; Guerrieri, R. Run-time detection and correction of heliostat tracking errors. *Renewable Energy*, 2017, 105, 702-711.

[25] Fathabadi, H. Novel high efficient offline sensorless dual-axis solar tracker for using in photovoltaic systems and solar concentrators. *Renewable Energy*, 2016, 95, 485-494.

[26] Natarajan, M.; Srinivas, T. Experimental and simulation studies on a novel gravity based passive tracking system for a linear solar concentrating collector. *Renewable Energy,* 2017, 105, 312-323.

[27] Lu, J.; Hajimirza, S. Optimizing sun-tracking angle for higher irradiance collection of PV panels using a particle-based dust accumulation model with gravity effect. *Solar Energy,* 2017, 158, 71-82.

[28] Cooper, P.L. The absorption of radiation in solar stills. *Solar Energy,* 1969, 12, 333-346.

[29] Stanciu, C.; Stanciu, D. Optimum tilt angle for flat plate collectors all over the World – A declination dependence formula and comparisons of three solar radiation models. *Energy Conversion and Management,* 2014, 81, 133-143.

[30] Soulayman, S. Comments on 'Optimum tilt angle for flat plate collectors all over the World – A declination dependence formula and comparisons of three solar radiation models' by Stanciu, C., Stanciu, D. *Energy Conversion and Management,* 2015, 93, 448-449.